2010

Linear Matrix Inequalities Based on Linear Quadratic Regulator for the H2/Hinf Control of the Inverter Split Air Conditioner Temperature

Yaubin Yang
Industrial Technology Research Institute

Min-Der Wu
Industrial Technology Research Institute

Yu-Choung Chang
Industrial Technology Research Institute

Linear Matrix Inequalities Based on Linear Quadratic Regulator for the H2/Hinf Control of the Inverter Split Air Conditioner Temperature

YauBin YANG[1]*, Min-Der WU[2], Yu-Choung CHANG[3]

[1]Industrial Technology Research Institute, Energy & Environment Research Lab.,
Chutung, Hshichu, Taiwan
(+886 3 591 4302, +886 3 582 0250, yaubinyang@itri.org.tw)

[2]Industrial Technology Research Institute, Energy & Environment Research Lab.,
Chutung, Hshichu, Taiwan
(+886 3 591 5077, +886 3 582 0250, MinDerWu@itri.org.tw)

[3]Industrial Technology Research Institute, Energy & Environment Research Lab.,
Chutung, Hshichu, Taiwan
(+886 3 591 3367, +886 3 582 0250, yuchoung@itri.org.tw)

* Corresponding Author

ABSTRACT

In the multi-evaporator air conditioners systems, the compressor speed and the expansion value opening degree affect coupling the evaporator wall temperature in two-phase region and the superheat on the evaporator tube. This research used system identification to get the inner & outer loop transfer functions between the air-conditioner and its environment. The anti-windup method avoided the saturation phenomenon generated from integral controller. The linear matrix inequalities (LMI) based on linear quadratic regulator (LQR) mixed H2 and Hinf control algorithm computed the optimal control gains from the input and state performance indexes. In the target temperature achievement example for the inverter split air conditioner, this proposed method controlled the air conditioner with two evaporator temperatures efficiently through those two optimal feedback gains. In addition, the results show a novel path for energy saving by the proposed LMI method.

1. INTRODUCTION

For the inverter split air conditioner, the indoor temperature was controlled by the evaporator temperature and the superheat. And the evaporator temperature and the superheat were controlled by the compressor speed and the several electronic expansion valves opening degree. The control for multi-input multi-output systems (MIMO) was well-known much more difficult than that for single input single output systems (SISO) because of the coupling effects especially for split air conditioner units. Lin and Yeh (2007) used decoupled control scheme for temperature control of multi-evaporators air conditioning systems based on system modeling and identification. Yakubovich (1962) provided the first solution for matrix inequalities. The multiple-input multiple-output linear matrix inequality algorithm got more attraction in recent years (Palhares et al., 1996; De Oliveira et al, 2002). This proposed study based on LMI algorithm achieved the target temperature from evaporator temperature and superheat adjustment by controlling compressor speed and electronic expansion valve opening degree. This study investigated the temperature control for air conditioners based on linear matrix inequalities algorithm. The paper is organized as follows. Section 2 presents brief review for inverter air-conditioning system. Section 3 presents the transfer function from system indemnification. Section 4 presents the anti-windup and section 5 shows LMI formulations. Section 6 presents several numerical results for the proposed approaches.

2. BRIEF REVIEW FOR INVERTER AIR-CONDITIONING SYSTEM

The air-conditioner contains four major parts: outdoor unit contains the compressor, condenser, electronic expansion valve and outdoor fan; indoor unit contains the evaporator and the indoor fan. Its operation cycle structural functions are as follows: (a) the compressor: the compressor with the permanent magnet brushless motor compresses the low-pressure low-temperature gaseous refrigerant into high-pressure high-temperature gaseous refrigerant. The refrigerant flow can be controlled by the compressor speed, and its speed is set to 15 ~ 90 Hz; (b) the condenser: the outdoor fan removes heat from the condenser to the outdoor atmosphere, so the high-pressure high-temperature gaseous refrigerant becomes the high-pressure middle-temperature liquid refrigerant; (c) the electronic expansion valve: the electronic expansion valve converts the high-pressure middle-temperature liquid refrigerant into the low-pressure low-temperature liquid refrigerant. The level of lower temperature and pressure can be controlled by the electronic expansion valve opening, and the opening degree is set to 10 ~ 500 Pulse; (d) the evaporator: the low-pressure low-temperature liquid refrigerant through the inhaled higher indoor temperature air evaporates into low-pressure low-middle-temperature gaseous refrigerant. In the meantime, this inhaled relatively higher indoor temperature air cools down and discharges back into the room, so that the indoor ambient temperature can go down into the required temperature. The low-pressure low-middle-temperature gaseous refrigerant at the evaporator export re-enters the compressor. One whole air-conditioner cycle is completed by those procedures.

The entrances and exports of the evaporator are in the two-phase coexistence of low-temperature liquid and low-middle-temperature gaseous refrigerant. The refrigerant from the evaporator export to the compressor entrance can be reheated by the ambient temperature, and this reheat procedure makes low-middle-temperature gaseous refrigerant overheat.

The low-pressure low-temperature liquid refrigerant through the evaporator in isothermal state becomes low-pressure low-temperature gaseous refrigerant working region, a liquid-gas two-phase coexistence saturation zone. If the refrigerant is heating up continually, then the refrigerant working region will leave the saturation zone and enter the overheated gaseous zone. The increased temperature which the evaporated low-pressure low-temperature refrigerant leaves the saturated zone and keeps heating up on the working region before entering the compressor is defined as the superheat T_{sh}.

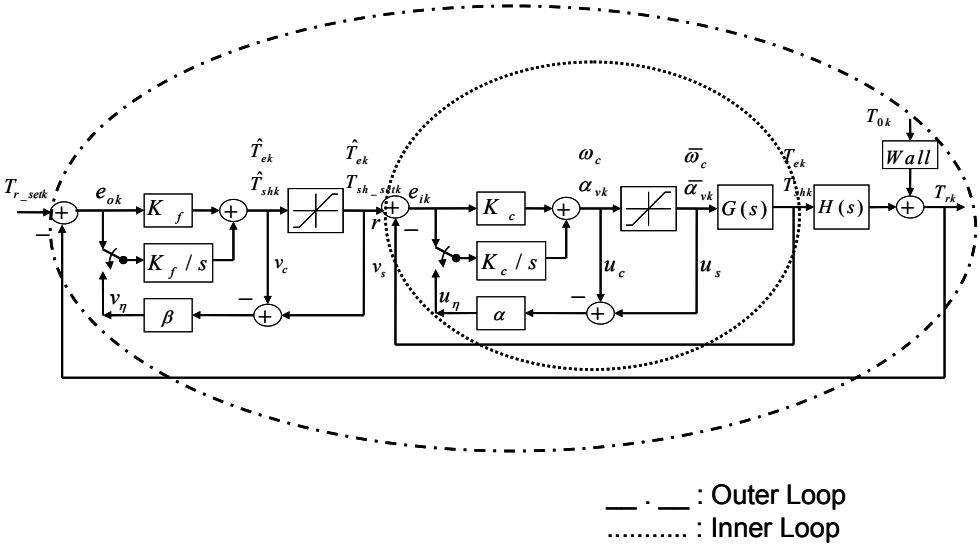

Figure 1: Inverter air-conditioner system control flow chart

The reaction rate of the inner loop and the outer loop was different, so this study discussed two feedback loops. The inner loop defined the relationship between the compressor and the multiple evaporators, and the outer loop defined the relationship between the multiple evaporators and the environment. The notation subscript k means from 1 to k and the number of multiple evaporators is k. For example, the evaporator temperatures T_{ek} means $[T_{e1} \;\; T_{e2}]'$ and two evaporators in this paper.

The indoor temperatures T_{rk} were generated by the evaporator temperatures T_{ek} and the superheats T_{shk} . The outer loop feedback errors e_{ok} between the indoor settings temperatures T_{r_setk} and the indoor temperatures T_{rk} were multiplied by the controller feedback gain K_f to get the evaporator temperatures $\hat{T}_{ek}$ and the superheats $\hat{T}_{shk}$. The high superheat makes the compressor damage easily, so the superheat values $\hat{T}_{shk}$ must be greater than superheat setting values T_{sh_setk} . The outer feedback gain K_f needs the anti-windup to avoid integrator saturation.

The evaporator temperatures T_{ek} and the superheats T_{shk} were generated by new compressor speed $\overline{\omega}_c$ and new electronic expansion valves $\overline{\alpha}_{vk}$. The inner loop feedback error e_{ik} between ($\hat{T}_{ek}$, $\hat{T}_{sh\_setk}$) from outer loop and (T_{ek} , T_{shk}) from inner loop were multiplied by the controller feedback gain K_c to get compressor speed ω_c and electronic expansion valve openings α_{vk} . The inner feedback gain K_c needs the anti-windup to avoid integrator saturation.

The high compressor speed makes the whole system damage easily, so the compressor speed must be less than new compressor speed $\overline{\omega}_c$. Those procedures based on the two feedback control gains make the split type air conditioner achieve the target temperature.

Indoor temperature changes were much slower than the outdoor unit. The proposed method handled them separately and made indoor temperature control efficiency. In the multiple-input multiple-output inverter air-conditioning system, the cooling fan speed of indoor unit and outdoor unit was set to be constant; the compressor speed ω_c and electronic expansion valve openings α_{vk} were set to the controllable inputs; the evaporator temperatures T_{ek} and the superheats T_{shk} were set to the outputs. The system control flow chart was shown in figure 1.

3. TRANSFER FUNCTION FROM SYSTEM IDENTIFICATION

3.1 System Identification

The evaporator is the exchange place between air-conditioner temperature and indoor temperature. X. D. He et al (1995) established equivalent vapor compression cycle dynamic parameters, and discussed evaporator model through the two-phase region and the superheat zone. The outer and inner loops are the multiple-input multiple-output parameter system, and the system identification transfer functions are shown in Figure 2. In Figure 2 (a), the compressor speed ω_c and the electronic expansion valve opening degrees α_{vk} are inputs, and the evaporator temperatures T_{ek} and the superheats T_{shk} which affect heat absorptive capacity in the evaporator are outputs. In Figure 2 (b), the evaporator temperatures T_{ek} and the superheats T_{shk} are inputs, and the indoor temperatures T_{rk} are output. Since the system identification is for MIMO system, the space state form systems can be expressed as

$$y = \begin{bmatrix} T_{e_k} \\ T_{sh_k} \end{bmatrix} = \left[G(s)_{(2k)\times(1+k)} \right] \begin{bmatrix} \omega_c \\ \alpha_{v_k} \end{bmatrix} = GX \; ; \; z = \left[T_{r_k} \right] = \left[H(s)_{(k)\times(2k)} \right] \begin{bmatrix} T_{e_k} \\ T_{sh_k} \end{bmatrix} = Hy \quad (1)$$

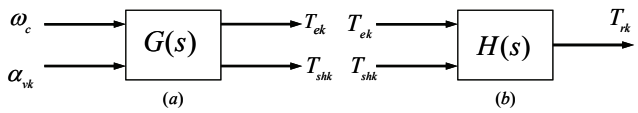

Figure 2: MIMO parameters block diagram

The transfer function estimation G of mth data by the least squares method shows,

$$\hat{G}_m = (X_m^T X_m)^{-1} X_m^T y_m \quad (2)$$

The $(m+1)^{th}$ data can be expressed as $y_{m+1} = X_{m+1} G$, so the transfer function estimation G is

$$\hat{G}_{m+1} = (X_{m+1}^T X_{m+1})^{-1} X_{m+1}^T y_{m+1} = (X_m^T X_m + x_{m+1}^T x_{m+1})^{-1} X_{m+1}^T y_{m+1} \tag{3}$$

After calculations and rearrangement, the recursive least squares equation is

$$\hat{G}_{m+1} = \hat{G}_m + (X_m^T X_m)^{-1} x_{m+1} \left[I + x_{m+1}^T (X_m^T X_m)^{-1} x_{m+1} \right]^{-1} \left[y_{m+1} - x_{m+1} \hat{G}_m \right] \tag{4}$$

The transfer function estimation H has similar equation 4 form.

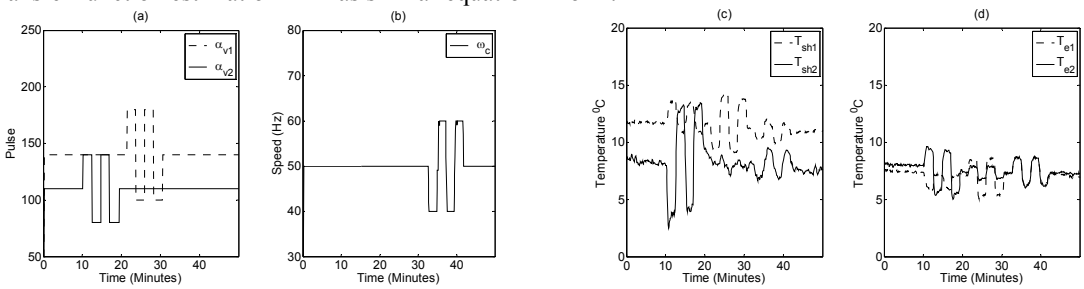

Figure 3: system identification for inner loop

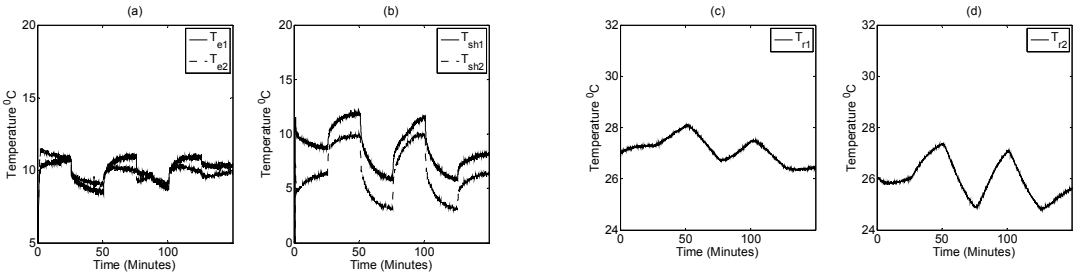

Figure 4: system identification for outer loop

For the inner loop, the compressor speed, the first electronic expansion valve opening and the second electronic expansion valve opening were fixed at 50 Hz, 140 Pulse and 110 Pulse respectively. First, the first electronic expansion valve opening degree changed from 100 to 180 Pulse. Second, the second electronic expansion valve opening degree changed from 80 to 140 Pulse. Finally, the compressor speed changed from 40 to 60 Hz. Each period took 4.5 minutes, and there were 2.25 minutes between two periods. The other two parameters remained constant while one parameter varied with time.

For the outer loop systems identification, the first evaporator remains 10.5 ^{0}C and superheat changed from 5 to 12 ^{0}C. The second evaporator remained 10 ^{0}C and superheat changed from 3 to 10 ^{0}C. Each period took 50 minutes.

The area of first room was around 48 m^2 and the area of second room was around 26 m^2. The height of the room was around 2.7 m. Figure 2 showed the MIMO parameters block diagram for outer and inner loops, figure 3 was the system identification for inner loop and figure 4 was the system identification for outer loop. The system identification by recursive least squares method was the first-order low-pass filter shown in equation 5.

$$G(s) = \begin{bmatrix} \frac{-0.0040}{s+0.0351} & \frac{0.0015}{s+0.0351} & \frac{-0.0006}{s+0.0351} \\ \frac{0.0017}{s+0.0228} & \frac{-0.0016}{s+0.0228} & \frac{0.0011}{s+0.0228} \\ \frac{-0.0048}{s+0.0308} & \frac{0.0003}{s+0.0308} & \frac{0.0018}{s+0.0308} \\ \frac{0.0049}{s+0.0279} & \frac{-0.0002}{s+0.0279} & \frac{-0.0043}{s+0.0279} \end{bmatrix} \quad H(s) = \begin{bmatrix} \frac{-0.00002}{s+0.0008} & 0 & \frac{0.00016}{s+0.0008} & 0 \\ 0 & \frac{-0.00025}{s+0.0015} & 0 & \frac{0.00065}{s+0.0015} \end{bmatrix} \tag{5}$$

4. ANTI-WINDUP

The integrator reduces the system steady-state error but the integrator saturation causes the windup phenomenon. In equation 6, the parameter u_s has three possible outputs corresponding to the controller input u_c.

$$u_s = \begin{cases} u_{\min} & \text{for} \quad u_c < u_{\min} \\ u_c & \text{for} \quad u_{\min} < u_c \le u_{\max} \\ u_{\max} & \text{for} \quad u_c > u_{\max} \end{cases} \tag{6}$$

In figure 1, the difference between u_s and u_c multiplies by coefficient α, then adds the error signal e is the input of integrator. This anti-windup can suppress integrator saturation phenomenon caused by integrator. In general, the bigger α value, the faster saturation convergent rate. A variable-structure (switching) for proportional integral anti-windup method was introduced (VSPI) (Hodel and Hall, 2001), i.e. $u_\eta = 0$ with $u_c = -Kx + r$ is in linear operation, and $u_\eta = -\alpha(u_c - u_s)$ with $u_c = -Kx + r$ is in saturation.

5. LMI formulation

5.1 Discrete time state space equations with anti-wind up for inverter split air conditioner systems

The system discrete time dynamic equation can be expressed as state space form,

$$X(k+1) = AX(k) + B_2 u_s(k) + B_\eta u_\eta(k) + B_1 w(k); \qquad z(k) = E_1 X(k) + E_2 u_s(k) + Gw(k) \tag{7}$$

Where u is control input, w is disturbance input, z is the reference output, $u_\eta = 0$ with $u_c = -Kx + r$ is in linear operation, and $u_\eta = -\alpha(u_c - u_s)$ with $u_c = -Kx + r$ is in saturation.

5.2 Hinf Formulation

The control is the closed-loop system to minimize Hinf rank from the disturbance input w to the reference output z. A. J. Connolly pointed out the designed controller from the entire control with Hinf estimation can effectively reduce the transient response time and the steady-state error (Connolly, 1995).

If the transfer function of the system has bounded in equation 8, then

$$\|H\|_\infty^2 = \sup_{\omega \in R} \frac{\|z\|_2^2}{\|\omega\|_2^2} = \sup_{\omega \in R} \frac{\sum z^T z}{\sum \omega^T \omega} \le \gamma^2 \tag{8}$$

$J_1 = \sum_0^\infty (\gamma^2 w^T \omega - z^T z)$ Where γ is the bounded and J_1 is performance index

In the Lyapunov stability theory, the system is said to be asymptotic stable if there exists a symmetric matrix $P = P^T$ in equation 7.

It is assumed that function $V(k)$ is $x^T(k)Px(k)$, and feedback compensator $u(k)$ is $-Kx(k)$. The discrete Lyapunov equation can be expressed as follow,

$$\Delta V - \left[\gamma^2 w^T(k) w(k) - z^T(k) z(k)\right] < 0 \text{ Where } \Delta V = V(k+1) - V(k) \tag{9}$$

From Equation 9, in the linear operation,

$$\begin{bmatrix} X \\ w \\ r \end{bmatrix}^T \begin{bmatrix} \overline{\overline{A}}^T P \overline{\overline{A}} - P + \overline{\overline{E}}^T \overline{\overline{E}} & * & * \\ B_1^T P \overline{\overline{A}} & -(\gamma^2 I - B_1^T P B_1) & * \\ \overline{\overline{B}}_2^T P \overline{\overline{A}} & \overline{\overline{B}}_2^T P B_1 & \overline{\overline{B}}_2^T P B_2 \end{bmatrix} \begin{bmatrix} X \\ w \\ r \end{bmatrix} < 0 \tag{10}$$

$$w = (\gamma^2 I - B_1^T P B_1)^{-1} B_1^T P(\overline{\overline{B}} r + \overline{\overline{A}} X) \text{ Where } \overline{\overline{A}} = A - B_2 K,\ \overline{\overline{B}} = B_2 \text{ and } \overline{\overline{E}} = E_1 - E_2 K \tag{11}$$

In the saturation situation,

$$\begin{bmatrix} X \\ u_s \\ w \\ r \end{bmatrix}^T \begin{bmatrix} \overline{\overline{A}}^T P\overline{\overline{A}} - P + E^T E & * & * & * \\ \overline{\overline{B}}_2^T P\overline{\overline{A}} & \overline{\overline{B}}^T P\overline{\overline{B}}_2 & * & * \\ B_1^T P\overline{\overline{A}} & B_1^T P\overline{\overline{B}}_2 & -(r^2 I - B_1^T PB_1) & * \\ -\alpha B_\eta^T P\overline{\overline{A}} & -\alpha B_\eta^T P\overline{\overline{B}}_2 & -\alpha B_\eta^T PB_1 & \alpha^2 B_\eta^T PB_\eta \end{bmatrix} \begin{bmatrix} X \\ u_s \\ w \\ r \end{bmatrix} < 0 \tag{12}$$

$$w = (\gamma^2 I - B_1^T PB_1)^{-1} B_1^T P((\overline{\overline{B}}u_s - \alpha B_\eta r) + \overline{\overline{A}}X) \text{ Where } \overline{\overline{A}} = A + \alpha B_\eta K \text{ , } \overline{\overline{B}} = B_2 + \alpha B_\eta \text{ and } \overline{\overline{E}} = E_1 \tag{13}$$

5.3 H2 Formulation

Choose performance index J_2, so that $J_2 = \sum_0^\infty (x^T Qx + u^T Ru)$ Where $Q = E_1^T E_1$, and $R = E_2^T E_2$ (14)

In linear operation,

$$\begin{bmatrix} X \\ r \end{bmatrix}^T \begin{bmatrix} \overline{\overline{A}}^T P\overline{\overline{A}} - P + E_1^T E_1 + K^T E_2^T E_2 K & * \\ B_2^T P\overline{\overline{A}} - E_2^T E_2 K & B_2^T PB + E_2^T E_2 \end{bmatrix} \begin{bmatrix} X \\ r \end{bmatrix} < 0 \tag{15}$$

In saturation situation,

$$\begin{bmatrix} X \\ u_s \\ r \end{bmatrix}^T \begin{bmatrix} \overline{\overline{A}}^T P\overline{\overline{A}} - P + E^T E & * & * \\ \overline{\overline{B}}_2^T P\overline{\overline{A}} & \overline{\overline{B}}_2^T P\overline{\overline{B}}_2 & * \\ -\alpha B_\eta^T P\overline{\overline{A}} & -\alpha B_\eta^T P\overline{\overline{B}}_2 & \alpha^2 B_\eta^T PB_\eta \end{bmatrix} \begin{bmatrix} X \\ u_s \\ r \end{bmatrix} < 0 \tag{16}$$

5.4 Linear matrix inequality expression

The two important concepts were shown here before deviating linear matrix inequalities.

The first is the Schur complement: $M = \begin{bmatrix} Q & S \\ S^T & R \end{bmatrix} > 0 \Leftrightarrow R > 0, Q - SR^{-1}S^T > 0$ (17)

The second is the inverse matrix expression: $(A + BCD)^{-1} = A^{-1} - A^{-1}B(C^{-1} + DA^{-1}B)^{-1} DA^{-1}$ (18)

For the convenient computation, set $P = Y^{-1}$, and $Z = KY$:

There exists $Y = Y^T$ such that Hinf norm LMI in linear operation can be expressed as:

$$\begin{bmatrix} -Y & * & * & * & * \\ 0 & 0 & * & * & * \\ \overline{\overline{A}}Y & \overline{\overline{B}} & -Y & * & * \\ 0 & 0 & B_1^T & -\gamma^2 I & * \\ \overline{\overline{E}}Y & 0 & 0 & 0 & -I \end{bmatrix} < 0 \tag{19}$$

There exists $Y = Y^T$ such that Hinf norm LMI in saturation can be expressed as:

$$\begin{bmatrix} -Y & * & * & * & * & * \\ 0 & E_2^T E_2 & * & * & * & * \\ 0 & 0 & 0 & * & * & * \\ -\overline{\overline{A}}Y & -\overline{\overline{B}} & B_\eta & -Y & * & * \\ 0 & 0 & 0 & B_1^T & -\gamma^2 I & * \\ \overline{\overline{E}}Y & 0 & 0 & 0 & 0 & -I \end{bmatrix} < 0 \tag{20}$$

There exists $W = W^T$ and $Y = Y^T$ such that H2 norm LMI in linear operation can be expressed as:

The optimization problem $\min_{W,Y}(W)$ subject to $\begin{bmatrix} W & \overline{\overline{B}}^T \\ \overline{\overline{B}} & Y \end{bmatrix} > 0, Y > 0$, $\begin{bmatrix} -Y & * & * & * \\ 0 & E_2^T E_2 & * & * \\ \overline{\overline{A}}Y & \overline{\overline{B}} & -Y & * \\ E_1 Y + E_2 KY & 0 & 0 & -I \end{bmatrix} < 0$ (21)

There exists $W = W^T$ and $Y = Y^T$ such that H2 norm LMI in saturation can be expressed as:

The optimization problem $\min_{W,Y}(W)$ subject to $\begin{bmatrix} W & \overline{\overline{B}}^T \\ \overline{\overline{B}} & Y \end{bmatrix} > 0, Y > 0$, $\begin{bmatrix} -Y & * & * & * & * \\ 0 & E_2^T E_2 & * & * & * \\ 0 & 0 & 0 & * & * \\ \overline{\overline{A}}Y & \overline{\overline{B}} & -\alpha B_\eta & -Y & * \\ \overline{\overline{E}}Y & 0 & 0 & 0 & -I \end{bmatrix} < 0$ (22)

5. NUMERICAL RESULTS

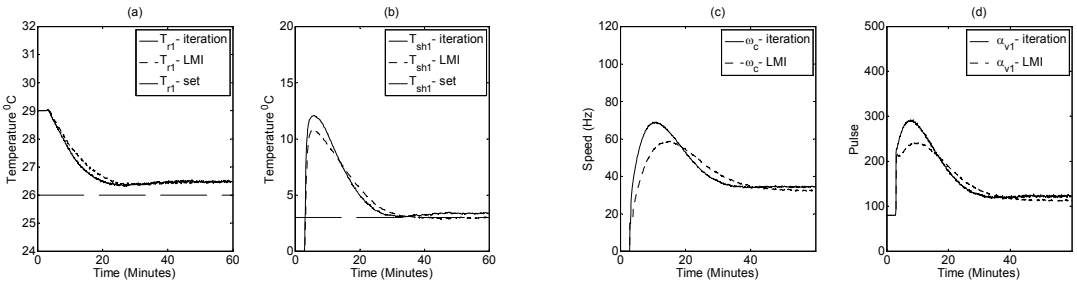

Figure 5 response comparisons for the first room

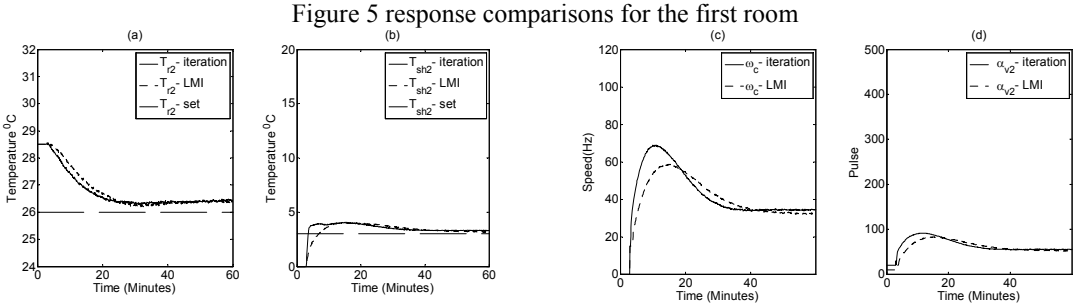

Figure 6 response comparisons for the second room

An inverter split air-conditioner operating condition was shown here. The outdoor temperature, first indoor room temperature, the second indoor room temperature, the compressor speed, first electronic expansion valve opening and the second electronic expansion valve opening were set to 31 ^{0}C, 29 ^{0}C, 28.2 ^{0}C, 15~ 90 Hz (600 rpm ~ 7200 rpm), 10 ~ 500 Pulse, and 10 ~ 500 Pulse, respectively. The indoor target temperature was determined to at 26 ^{0}C. The experimental machines are split type with R410A refrigerant, and the cooling capacities are 3.5kW and 5.0kW. The compressor speed and electronic expansion valve opening were the inputs; two-phase wall temperature and superheat were the outputs. This study was based on multiple-input multiple output (MIMO) system, so the evaporator temperature and superheat were cross-coupling controlled by compressor speed and electronic expansion valve opening at the same time.

Those MIMO simulated results based on mixed H2/Hinf LMI and traditional interaction scheme were shown in figure 5, 6. The indoor temperature result in figure 5, 6(a) was decreased gradually before they reached the steady state. The traditional iteration scheme was for validation purpose. Their steady state error temperatures for two indoor rooms were acceptable, says less than 0.5 ^{0}C. The dash line is for proposed LMI method and the solid line is for traditional iteration method. In figure 5, 6(c), the highest compressor speed for LMI was 17.6% less than that for

the traditional iteration method. The lower compressor speed the lower electric current usage. In figure 5, 6(d), for the electronic expansion valve opening, the LMI method was also less than the tradition iteration method. The less opening the little more electric current usage, but the effect of opening on current was less than that of compressor speed on current according to empirical investigation. The proposed LMI method provided a path for energy saving.

6. CONCLUSIONS

This paper presented a new approach for inverter split air conditioner. The inner and outer loop LMI separation schemes were first addressed here. The method didn't need to compute only one transfer function represent whole system. This proposed method could deal with the two loops separately in the same way, so the inner loop gain and outer loop gain were granted.

The results showed that multivariable temperature control system by linear matrix inequities was controllable and convergent. The control logic mentioned as follows: two indoor temperatures were controlled by two evaporator temperatures and two superheats. Those superheats were controlled immediately by the compressor speed and two electronic expansion valve opening degrees. Comparing the indoor temperature changes $T_{rk} - T_{r\_setk}$ with the superheat setting values T_{sh_setk} could control the indoor temperature effectively.

In the beginning of control, the room temperature was much larger than its target value, and superheat was at high state. The control system reduced superheat by the high compressor speed and high electronic expansion valve opening degree. When the room temperature was close to setting value, the superheat was at low state. The compressor speed and electronic expansion valve opening had also dropped to low speed and low openings. The system was operating under the steady state; the indoor temperature was stable under the control settings.

Comparing with the steady state superheat, the high superheat affected high speed compressor. The system increased energy use. The low superheat affected low speed compressor. The system decreased energy use. Figure 5, 6(b) showed the LMI method was better energy saving than traditional iteration method.

Until the indoor temperature setting values reached and the compressor speed and electronic expansion valve opening also became steady state. The LMI formulation guaranteed the computation time was much faster than the traditional iteration time. In addition, the compressor speed for LMI scheme was less than that for iteration scheme, so this method was also a novel energy saving approach, shown in figure 5, 6(c).

REFERENCES

Connolly, A. J., Green, M., Chicharo, J. F., and Bitmead, R. R., 1995, The design of LQG and controllers for use inactive vibration control and narrow band disturbance rejection, *Proc. 34th Conf. on Decision and Control, Vol. 3, pp. 2982-2987.*

De Oliveira, M. C., Geromel, J. C., and Bernussou, J., 2002, Extended and Norm Characterization and Controller Parameterization for Discrete-Time Systems, *Int. J. Control, vol. 75, no. 9, pp. 666-679.*

He, X. D., Liu, S., and Asada, H. H., 1995, Modeling of Compression Cycles for Advanced Controls in HVAC Systems, *Proc. American Control Conf., pp. 3664-3668.*

Hodel , A. S., and Hall, C. E., 2001, Variable-Structure PID control to Prevent Integrator Windup, *IEEE Transactions on Industrial Electronics, vol. 48, no. 2, pp. 442-451.*

Lin, J. L., and Yeh, T. J., 2007, Modeling, Identification and Control of Air-conditioning Systems, *Int. J. of Refrigeration, Vol. 30, No. 2, pp. 209-220.*

Palhares, R. M., Ramos, D. C. W. and Peres, L. D., 1996, Alternate LMIs Characterization of and Central Discrete-Time Controllers, *Proc. of the 35th Conf. on Decision and Control, Koba, Japan, pp. 1495-1496.*

Yakubovich,V.A., 1962, The solution to certain matrix inequalities in automatic control, *Dokl. Akad. Nauk USSR 143 (1962), pp. 1304–1307*

ACKNOWLEDGEMENT

The authors gratefully acknowledge the financial support provided by the Bureau of Energy, Ministry of Economic Affairs, Taiwan, R. O. C.